Structural and electronic properties of $(3\sqrt{2}\times\sqrt{2})R45°$-Sn/Cu(100): Density functional theory and scanning tunneling microscopy

J. D. Fuhr,[1] J. E. Gayone,[1] J. Martínez-Blanco,[2] E. G. Michel,[2] and H. Ascolani[1]
[1]*Centro Atómico Bariloche, CNEA, and CONICET, Av. E. Bustillo 9500, R8402AGP Bariloche, Argentina*
[2]*Departamento de Física de la Materia Condensada and Instituto Universitario de Ciencia de Materiales "Nicolás Cabrera," Universidad Autónoma de Madrid, 28049 Madrid, Spain*

(Received 11 May 2009; revised manuscript received 6 August 2009; published 10 September 2009)

The structural and electronic properties of the $(3\sqrt{2}\times\sqrt{2})R45°$ phase of 0.5 monolayers of Sn on Cu(100) have been investigated using a combination of scanning tunneling microscopy experiments and total-energy-minimization calculations. Theory and experiment support the missing-row surface-alloy structure as the ground state for this surface [K. Pussi, E. Al Shamaileh, E. McLoughin, A. A. Cafolla, and M. Lindroos, Surf. Sci. **549**, 24 (2004)]. The calculated electronic structure reproduces almost perfectly both the experimental scanning tunneling microscopy images and the observed electronic bands. Our results conclusively indicate that the creation of Cu vacancies in the top surface layer produces a significant reduction of the total energy. We also report a metastable $(3\sqrt{2}\times\sqrt{2})R45°$ phase coexisting with the ground state at room temperature, which we attribute to a two-missing-row surface-alloy structure.

DOI: 10.1103/PhysRevB.80.115410 PACS number(s): 73.20.At, 68.37.Ef, 68.35.Rh

I. INTRODUCTION

Surface reconstructions and phase transitions have received ample attention, both from theoretical and experimental points of view.[1,2] As in the case of low-dimensional materials, the surfaces of crystals are expected to exhibit collective phenomena with specific properties. Metal monolayers deposited on top of another metal or of a semiconductor are beginning to show this broad range of complex phenomena, including charge-density waves (CDWs),[3] Mott transitions,[4] or strong correlation in narrow surface resonances[5] among others. Metal monolayers deposited on Cu(100) have deserved ample attention during recent years as model systems to understand surface CDWs.[6–13] A CDW is a charge-ordered state with very interesting properties because it represents an accessible macroscopically coherent state.[14,15] In the CDW state, the lattice reorders slightly at expenses of the elastic energy, giving rise to a periodic lattice distortion and a new supercell. The loss of elastic energy is compensated in the new supercell by a gain in electronic energy because the electronic bands are more favorable from the energetic point of view. This is usually achieved through the opening of a band gap $2W$. The structural distortion is usually related to a soft phonon. Due to this fact, a common way to understand the properties of a particular CDW system is to compare the size of the electronic gap with respect to the phonon energies. There are two limiting cases well described by theory, corresponding to an electronic gap $2W$ comparable to phonon energies (weak-coupling limit with long coherence) and to an electronic gap much larger than phonon energies (strong-coupling limit with small coherence). Aruga[16] recently proposed that metal monolayers on (100) surfaces of noble metals could represent a new paradigm for surface charge-density wave systems, characterized by a strong coupling with long coherence. In this paper, we focus on one of these cases, the $(3\sqrt{2}\times\sqrt{2})R45° \Leftrightarrow (\sqrt{2}\times\sqrt{2})R45°$ (in short $3\sqrt{2}\Leftrightarrow\sqrt{2}$) phase transition observed at 360 K for 0.5 monolayers of Sn on Cu(100).[9] This case is especially interesting, as the condition $Q=2k_F$ is almost perfectly fulfilled. Moreover, an electronic gap opens in the nested regions of the Fermi surface of the high-temperature (HT) phase when the temperature decreases below 400 K,[9] i.e., only ~40 K above the structural critical temperature. Thus, there is a gapping-degapping transition almost at the structural critical temperature, as expected for a weak-CDW transition. However, the size of the gap observed in the $3\sqrt{2}$ low-temperature phase turned out to be at least 45 times larger than the value predicted for weak CDWs.[9,12] These features have also been reported for the phase transitions found in the In/Cu(100) and Pb/Cu(100) systems[8,10,16] and are typical of the new paradigm.

A detailed knowledge of both the electronic and the crystallographic structures of the involved low-temperature (LT) and HT phases is needed to disentangle the mechanism driving a phase transition. On the basis of a dynamical low-energy electron-diffraction (LEED) study, Pussi *et al.* proposed that the $3\sqrt{2}$ LT phase of 0.5 ML Sn/Cu(100) is a two-dimensional (2D) surface alloy.[17] As shown in Fig. 1(a), the model is characterized by the presence of a line of Cu vacancies along the [001] surface direction in the top atomic layer. We note that this model for the $3\sqrt{2}$ phase does not correspond to a simple distortion of an ordered $\sqrt{2}$ surface alloy with 0.5 ML of Sn atoms replacing Cu atoms in the top surface layer, as one would expect if it were a Peierls-type phase transition [indeed, a Peierls-like distortion could be compatible with models (B) or (C) in Fig. 1 from Ref. 17]. This $3\sqrt{2}$ LT structure was studied by Martínez-Blanco *et al.*[18] using surface x-ray diffraction and the structural parameters found are in very good agreement with the "missing-row" (MR) LEED model by Pussi *et al.*

In this paper, we set out to investigate the crystallographic and electronic structures of the $3\sqrt{2}$ phase and specially the possible existence of Cu vacancies. To this end, we combined scanning tunneling microscopy (STM) experiments with a complete program of total-energy-minimization calculations based in the density-functional theory (DFT).

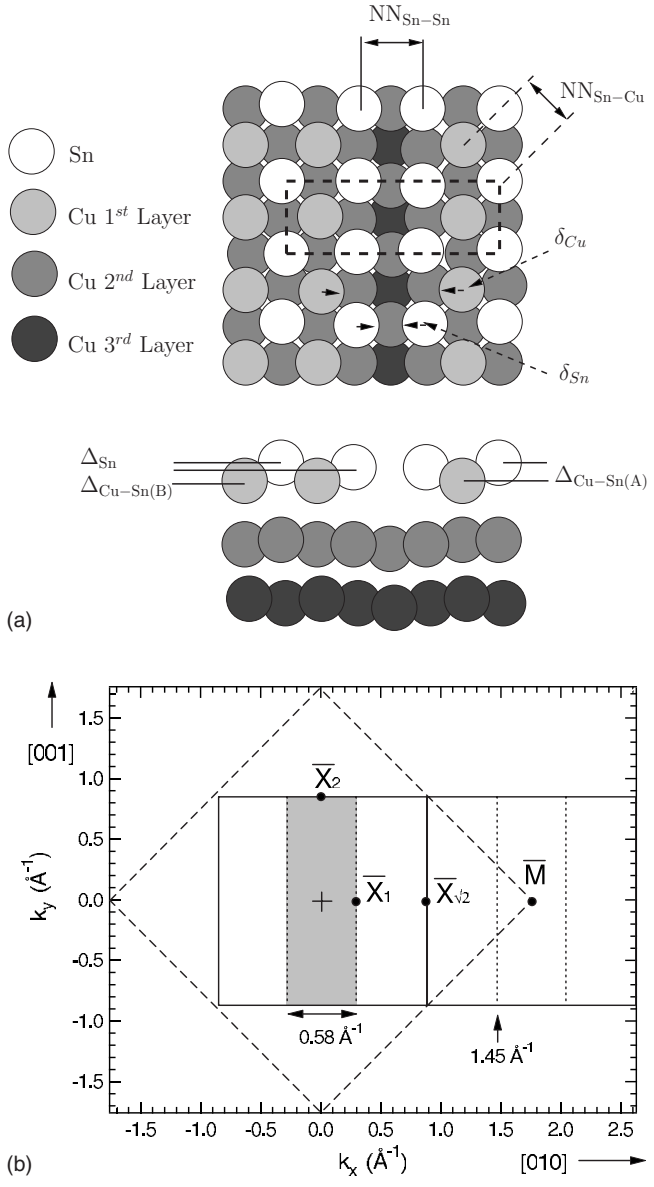

FIG. 1. (a) Schematic representation of the MR model from Ref. 17 for the $3\sqrt{2}$ phase. Notice the line of Cu vacancies parallel to the [001] crystallographic direction in the top atomic layer. (b) Reciprocal space of the 0.5 ML Sn/Cu(100) interface: dashed lines, (1×1) Brillouin zone; continuous lines: $\sqrt{2}$ Brillouin zone; dotted lines, $3\sqrt{2}$ Brillouin zone (one of them shaded for clarity).

II. EXPERIMENTAL DETAILS AND THEORETICAL METHODS

The Cu(100) substrate (from Surface Preparation Laboratory, SPL) was prepared by repeated cycles of argon bombardment and annealing at 800 K. The $3\sqrt{2}$ phase was produced by evaporating Sn from a home-made Knudsen cell on a clean Cu(100) surface at room temperature (RT) and at pressures lower than 3.10^{-9} mbar. One monolayer (ML) is defined in this paper as the atomic surface density of the bulk Cu(100) surface, i.e., 1.54×10^{15} at/cm^2. The evaporation rate was calibrated from the sequence of phases formed below 1 ML.[19,20] We usually obtained sharp $3\sqrt{2}$ LEED patterns which eventually improved after annealing the sample at 450 K. The STM images were taken with a commercial microscope (Omicron) at the surface physics laboratory of the Centro Atómico Bariloche.

The DFT calculations were performed using the QUANTUM-ESPRESSO package,[21] which is an implementation of the plane-wave with ultrasoft pseudopotentials[22] approach. For the exchange-correlation term, we used the generalized-gradient approximation (GGA) as given by the Perdew-Wang (PW91) functional.[23] For the surface calculations we have used the slab method, with seven Cu layers representing the surface and an equivalent vacuum size of another seven layers. Except for the two lower layers that were kept fixed at the bulk distance, all the atoms in the cell were allowed to relax. We used a wave-function/charge cutoff of 25/200 Ry and Brillouin integrations were done using $15\times15\times1$ and $5\times15\times1$ grids for the $\sqrt{2}$ and the $3\sqrt{2}$ structures, respectively. The theoretical STM images shown in this paper were calculated within the Tersoff-Hamann approximation.[24]

III. RESULTS

A. DFT calculations

Two aspects should be considered in order to determine the structure of the $3\sqrt{2}$ LT phase: the possible formation of a surface alloy and the presence of Cu vacancies. In order to investigate the first issue, we considered the following two possible crystallographic structures with $\sqrt{2}$ periodicity and 0.5 ML of Sn atoms: (i) an overlayer of Sn atoms adsorbed in fourfold hollow sites of the Cu(100) surface and (ii) an ordered surface alloy where the Sn atoms replace half of the Cu atoms in the top layer. These $\sqrt{2}$ structures are schematically shown in Figs. 2(a) and 2(b). As we shall show below, our theoretical results strongly support surface-alloy formation. For this reason, we considered for the $3\sqrt{2}$ LT phase only surface-alloy structures with 0.5 ML of Sn atoms, namely, the MR model of Pussi *et al.* shown in Fig. 2(d) [and in Fig. 1(a)], a two-missing-row (2MR) structure illustrated in Fig. 2(c), and a distorted $\sqrt{2}$ surface-alloy structure[25] (not shown) which turned out to relax to the undistorted $\sqrt{2}$ surface alloy.

We define the adsorption energy per Sn atom as

$$E_{ads} = -\left(\frac{E_{slab} + (N_{vac} + N_{subs})E_{Cu} - E_{sup}}{N_{Sn}} - E_{Sn}\right), \quad (1)$$

where E_{slab} is the total energy of the slab with the adsorbed Sn atoms, E_{sup} is the total energy of a slab corresponding to a clean surface with the same area, N_{Sn} is the number of Sn atoms in the unit cell, E_{Sn} is the Sn atomic-energy reference, N_{vac} is the number of Cu vacancies, and N_{subs} is the number of Sn atoms substituting Cu atoms. For both the $\sqrt{2}$ surface alloy and the $3\sqrt{2}$ superstructures, we have taken into account that there are $(N_{vac}+N_{subs})$ less Cu atoms than in the clean surface by adding the corresponding Cu bulk energy (E_{Cu}).

From the energetic point of view, the surface alloy, with an adsorption energy of −3.94 eV per Sn atom, is more fa-

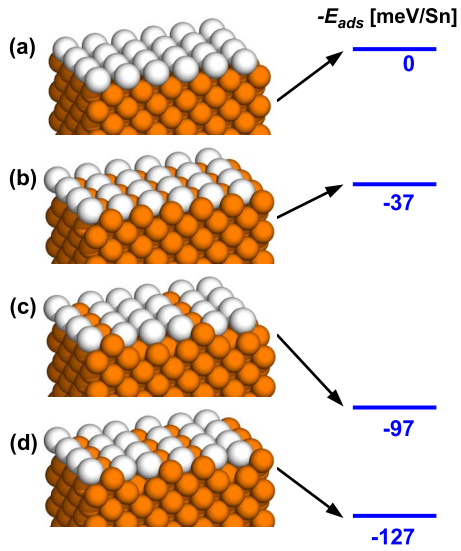

FIG. 2. (Color online) Schematic illustration of the four structural models analyzed in this work for the 0.5 ML Sn/Cu(100) interface. Structures in (a) and (b) correspond to the overlayer and the ordered surface-alloy $\sqrt{2}$ models, respectively, while those in (c) and (d) correspond to $3\sqrt{2}$ surface-alloy reconstructions. In particular, model (c) is the metastable 2MR structure observed in this work (see text for details) and model /9d) is the MR structure proposed by Pussi *et al.* (Ref. 17). The right energy scale shows the adsorption energy per surface Sn atom corresponding to each structure, taking the overlayer model as the zero of energy.

vorable than the overlayer configuration by −37 meV per Sn atom. The electronic bands obtained for these two $\sqrt{2}$ configurations along the $\overline{\Gamma X}_{\sqrt{2}}$ line of the Brillouin zone are shown in Fig. 3, where the size of each circle is proportional to the weight of the corresponding state on the surface Sn atoms. The corresponding reciprocal space is illustrated in Fig. 1(b). A visual inspection of the results shown in Fig. 3 reveals that there is an important difference between the bands obtained for these two $\sqrt{2}$ configurations: only the surface alloy exhibits an electronic band with a large weight on

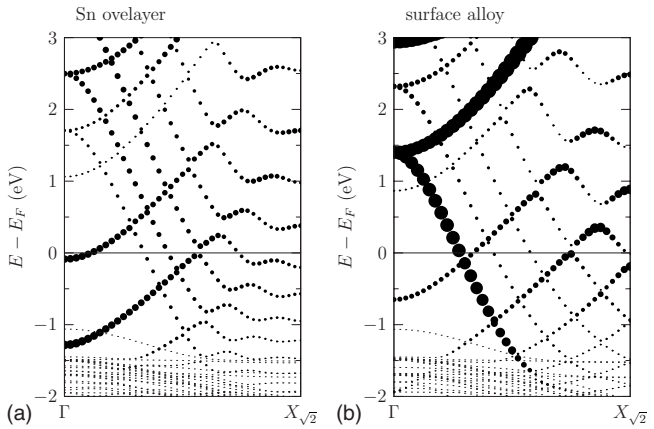

FIG. 3. Band structures along [010] direction for the two $\sqrt{2}$ configurations: (a) Sn overlayer and (b) surface alloy. Reciprocal space high-symmetry points are defined in Fig. 1(b). The size of each circle is proportional to the weight of the corresponding state on the Sn atoms.

the Sn atoms, i.e., a surface state. This dramatic difference between the two $\sqrt{2}$ configurations suggests that the Sn-Sn distance (3.61 Å) is too large to give rise to a significant interaction between Sn orbitals. This explains why the overlayer configuration does not develop a surface state. We note that Gao *et al.* arrived to a similar conclusion for a $\sqrt{2}$ overlayer of 0.5 ML of In deposited on Cu(100).[26] In their calculation a surface state was found only for a bilayer of In atoms, where the interatomic distance is much smaller. On the other hand, the Sn-Cu distances in the case of the surface-alloy configuration are short enough to give rise to significant interactions and, thus, to produce a surface state.

In the experimental results of Ref. 9, the $\sqrt{2}$ HT phase of the 0.5 ML Sn/Cu(100) interface shows a surface band, *S*, whose dispersion follows the Cu *sp* bulk band. The surface band is observed in the bulk band gap around $\bar{M}$ point but also outside it. The dispersion of *S* follows a parabola with an effective mass $m^*=1.3\ m_e$ (m_e the electron mass). Along $\overline{\Gamma M}$ direction, the surface band crosses the Fermi level E_F at 1.46 and 2.01 Å^{-1}. These crossing points coincide with the Brillouin-zone edges of the $3\sqrt{2}$ superstructure centered at the $\bar{M}$ point, as seen in Fig. 1(b). This means that the two crossing points along $\overline{\Gamma M}$ direction span a $2k_F$ vector equal to the periodicity of the $3\sqrt{2}$ phase along the same direction. The calculated surface band obtained for the ordered $\sqrt{2}$ surface alloy [Fig. 3(b)] shows a remarkable agreement with the experimental surface band *S*. In order to compare *S* with the calculated band, it is convenient to fold the experimental band into the first $\sqrt{2}$ Brillouin zone. This operation brings the two crossing points to $k_\parallel/k(\bar{X}_{\sqrt{2}})$ values of ± 0.32. Notice that these values are almost $\pm 1/3$, just the positions where the $\overline{\Gamma X}_{\sqrt{2}}$ line crosses the first Brillouin-zone edges of the $3\sqrt{2}$ superstructure. From the theoretical side, the calculated surface band obtained for the $\sqrt{2}$ surface alloy crosses E_F at $k_\parallel/k(\bar{X}_{\sqrt{2}})=0.28$.

Next, we investigated the possibility of a $3\sqrt{2}$ superstructure derived from the $\sqrt{2}$ surface alloy by slightly displacing the atoms from their $\sqrt{2}$ positions. We tried several different initial configurations, and in particular we moved up one of the three Sn atoms in the unit cell and approached the two remaining Sn atoms to each other. After relaxing the initial configurations, we always arrived to the same structure and adsorption energy, obtained for the $\sqrt{2}$ surface alloy. Therefore, we could not find any $3\sqrt{2}$ surface alloy with a 1:1 Sn:Cu ratio in the top layer (without Cu vacancies).

The $3\sqrt{2}$ MR structure was generated by removing one out of three lines of Cu atoms from the top surface layer of the ordered $\sqrt{2}$ surface alloy. From the total energy calculation, we obtained for this structure an adsorption energy per Sn atom of −4.03 eV, a value significantly lower (−90 meV per Sn atom) than the one obtained for the $\sqrt{2}$ surface-alloy model, as indicated in Fig. 2. Among the configurations considered in this study, the MR surface structure was found to be the one with lowest total energy. Table I shows the distances obtained for the relaxed structure. They are compared to the values of the structural parameters determined by Pussi *et al.*[17] from their dynamic LEED study of the $3\sqrt{2}$ phase and with those obtained by Martínez-Blanco

TABLE I. Distances obtained from our total-energy-minimization calculations for the $3\sqrt{2}$ MR structure compared to experimental values given by Pussi *et al.* (Ref. 17) and Martínez-Blanco *et al.* (Ref. 18). See Fig. 1(a) for the definition of the distances.

Distance	Ref. 17 [Å]	Ref. 18 [Å]	This work [Å]
Δ_{Sn}	0.12 ± 0.08	0.13 ± 0.03	0.12
$NN_{Sn\text{-}Sn}$	3.10 ± 0.10	3.08 ± 0.02	3.11
$NN_{Sn\text{-}Cu}$	2.59 ± 0.07	2.67 ± 0.03	2.66
$\Delta_{Cu\text{-}Sn(A)}$	0.39 ± 0.07	0.35 ± 0.03	0.53
$\Delta_{Cu\text{-}Sn(B)}$	0.27 ± 0.07	0.22 ± 0.02	0.41
δ_{Sn}	0.26 ± 0.10	0.27 ± 0.01	0.26
$\delta_{Cu(1)}$	0.01 ± 0.04	0.15 ± 0.03	0.13

et al.[18] from their surface x-ray diffraction study. As seen from Table I, the calculated parameters are in very good agreement with the corresponding experimental values, except for the Cu-Sn height differences ($\Delta_{Cu\text{-}Sn(A)}$ and $\Delta_{Cu\text{-}Sn(B)}$) which are slightly overestimated by the calculations.

Also, in order to investigate $3\sqrt{2}$ structures with different configurations of Cu vacancies, we considered the 2MR model depicted in Fig. 2(c). The 2MR model consists in a surface-alloy structure similar to the MR one but with two lines of Cu vacancies instead of only one. We note that the 2MR and MR models represent the only two possible surface-alloy configurations compatible with $3\sqrt{2}$ periodicity, 0.5 ML of Sn coverage, and Cu vacancies in the top surface layer. Interestingly, we obtained for the relaxed 2MR structure an adsorption energy per Sn atom of −4.0 eV, that is only 30 meV per Sn atom higher than the value obtained for the MR structure.

In conclusion, the results of our total-energy-minimization calculations, which are summarized in Fig. 2 and Table I, strongly support the MR surface-alloy model for the ground state of the $3\sqrt{2}$ LT phase. Then, our next step was to compare the electronic surface bands calculated for the relaxed MR structure to those measured on the $3\sqrt{2}$ LT phase using angle-resolved photoemission spectroscopy (ARPES) by Martínez-Blanco *et al.*[9,12] In Fig. 4(a) we show the band structure obtained for the $3\sqrt{2}$ MR structure determined theoretically in this work along the two now nonequivalent $\overline{\Gamma X}_1$ and $\overline{\Gamma X}_2$ directions. As before, the sizes of the circles are proportional to the weight of each state on the surface Sn atoms. Note that the bigger unit cell implies 3 times more bands than for the $\sqrt{2}$ structure.

Before analyzing the calculated bands, we summarize the main features of the experimental surface bands of the $3\sqrt{2}$ LT phase, reported in Refs. 9 and 12. Along $\overline{\Gamma M}$ direction, the ARPES spectra show two intense surface bands around $\bar{M}$ point. One of the bands turned out to be indistinguishable from the *S* band observed in the $\sqrt{2}$ HT phase. The other band folded back at 1.45 $Å^{-1}$, which coincides with a $3\sqrt{2}$ Brillouin-zone edge, with a minimum binding energy of 0.7 eV. The observation of two surface bands is explained from the two-domain nature of the $3\sqrt{2}$ phase.

As shown in Fig. 4(a), the calculated bands along $\overline{\Gamma X}_2$ direction exhibit a S_1 state with a significant weight in the Sn atoms and with a dispersion similar to the surface band obtained for the ordered $\sqrt{2}$ surface alloy [see Fig. 3(b)]. On the other hand, a comparison of the calculated S_1 band with those observed in the $3\sqrt{2}$ LT phase experimentally indicates that it describes very well the dispersion of the experimental *S* band, i.e., the band that is indistinguishable from the band observed in the $\sqrt{2}$ HT phase. In particular, the calculated S_1 surface band crosses the Fermi level at $k_{\parallel}/k(\bar{X}_2)=0.30$, which compares very well with the crossing point of the *S* band at $k_{\parallel}/k(\bar{X}_2)=0.32$. We therefore associate the S_1 state with the *S* surface band of the $3\sqrt{2}$ LT phase. There is another surface state along the $\overline{\Gamma X}_2$ direction with a dispersion similar to that of the S_1 band. However, contrary to the S_1 state, it lies outside the bulk band gap making it difficult to observe experimentally. On the other hand, the bands along $\overline{\Gamma X}_1$ direction are very different. First, there is no surface state crossing the Fermi level. In addition, there is an occupied S_2 band with significant weight on the Sn atoms and a binding energy of $E_g \simeq 0.6$ eV at the border of the Brillouin zone. We associate the S_2 state with the surface state of the $3\sqrt{2}$ LT phase that folds back at 1.45 $Å^{-1}$ along $\overline{\Gamma M}$ direction.

In order to determine the absolute size of the electronic gap expected at 1.45 $Å^{-1}$ along $\overline{\Gamma M}$ direction, one should find the corresponding empty surface band. This surface band should exhibit an opposite dispersion, i.e., the energy should increase with decreasing $k_{\parallel}$. The best candidate for the upper band of the gap is the band with the correct dispersion beginning at X_1 with a binding energy close to the Fermi level, which we indicate with a dashed line in Fig. 4(a). This band has a rather small weight on the Sn atoms, probably because it is out of the gap and it mixes more strongly with bulk states, but it satisfies all the other requirements.

Experimental results from ARPES probe two-domain samples mostly in the $\bar{M}$ point band gap. Figure 4(b) shows the surface states identified in the theoretical calculations plotted in the reciprocal-space region where they are detected in the experiment and for two 90°-rotated domains of the $3\sqrt{2}$ surface alloy. In this figure, the surface states S_1 and S_2 observed in Fig. 4(a) have been unfolded, taking into account the periodicity of the $3\sqrt{2}$ superstructure. Gray areas correspond to the projection of calculated bulk bands on the (100) plane (without any surface folding). We note that our calculations reproduce correctly the bulk band gap around the $\bar{M}$ point of the Cu(100) Brillouin zone. The figure shows that the theoretical surface band found along $\overline{\Gamma X}_2$ direction follows the Cu *sp* bulk band edge, in excellent agreement with the experimental observations. Furthermore, the theoretical results shown in this figure reproduce almost perfectly the experimental bands reported in Fig. 2 of Ref. 9. Finally, we have also calculated the binding energy E_g of the surface state at the Brillouin zone edge as a function of the azimuthal angle ϕ with respect to the $\overline{\Gamma M}$ direction. The result appears in Fig. 4(c), which shows how the band approaches the Fermi energy as we move away from $\overline{\Gamma M}$ direction, and finally touches it for $\phi \simeq 13°$. This is again in excellent agreement with the experimental results reported in Fig. 3 from Ref. 9.

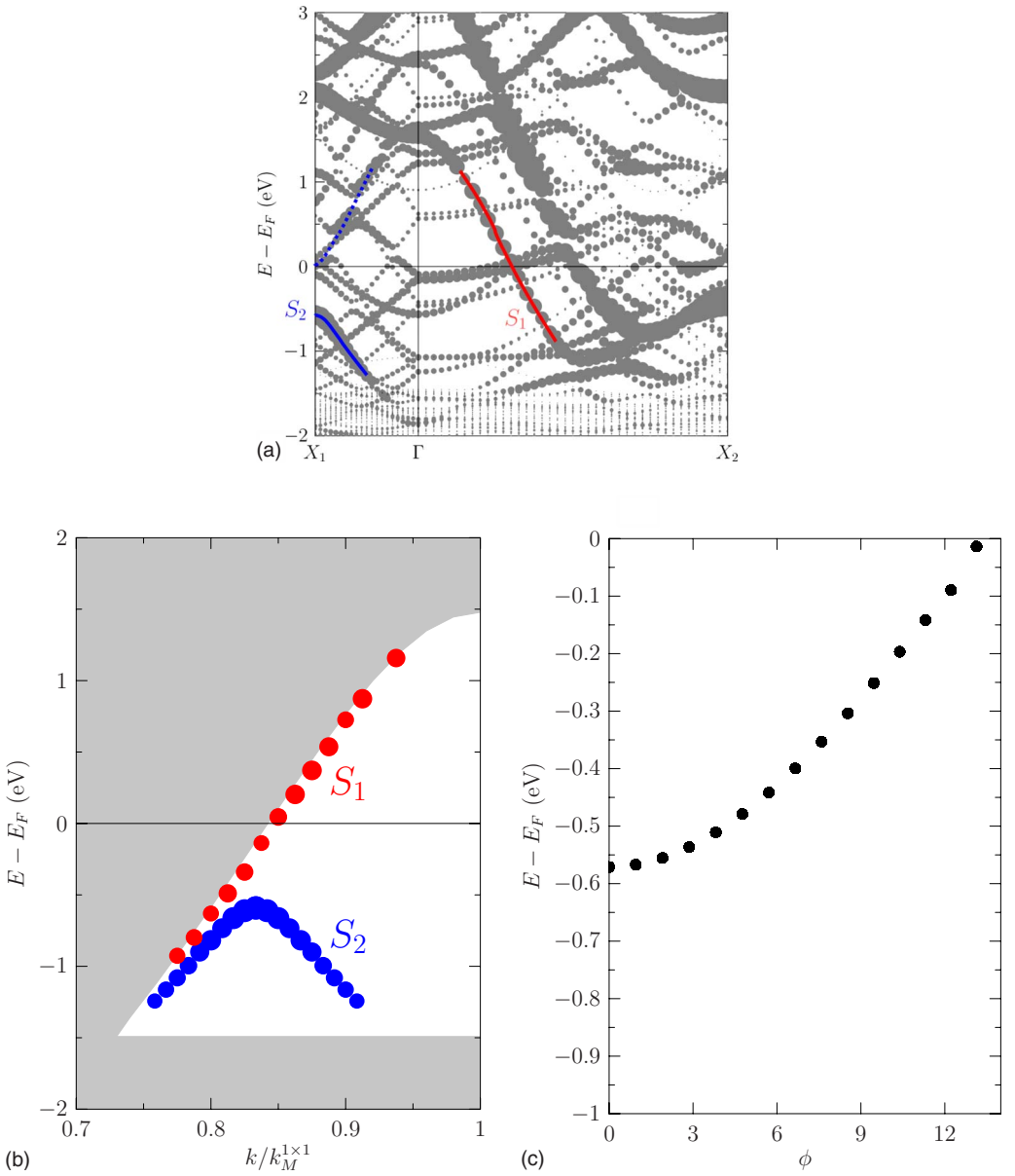

FIG. 4. (Color online) Calculated electronic structure of the $3\sqrt{2}$ MR structure determined theoretically in this work [see Fig. 1(a) and Table I]. (a) Band structure along the nonequivalent $\overline{\Gamma X}_1$ and $\overline{\Gamma X}_2$ directions. The size of the circles is proportional to the weight of each state in the Sn atoms. The lines indicate the identified surface states as explained in the text. (b) Surface states corresponding to the two 90°-rotated domains of the $3\sqrt{2}$ MR structure shown in the reciprocal-space region where they are observed experimentally in the $3\sqrt{2}$ LT phase. Gray areas correspond to the projection of calculated bulk bands on the (100) plane. (c) Energy E_g of the maximum of the surface state S_2 (measured from the Fermi energy) as a function of the azimuthal angle ϕ with respect to the ΓM direction.

B. STM images

In Fig. 5 we compare high-resolution STM images of the $3\sqrt{2}$ LT phase obtained at room temperature with simulated images corresponding to the MR structure determined theoretically in this work (fourth column of Table I). Figure 5(a) shows a filled-state image of a relatively large area of the surface where a perfectly ordered array of protrusions with $3\sqrt{2}$ periodicity is resolved. It is clear that one out of three rows of protrusions (oriented along a given [001] direction) has a larger apparent height. This is a typical feature of the $3\sqrt{2}$ phase, also observed in previous STM studies.[27] We observed that the experimental STM images of the $3\sqrt{2}$ phase were almost independent of the bias voltage, which suggests that the observed rumpling has a structural origin.

The STM image shown in Fig. 5(b) has a very good resolution and, therefore, it provides detailed information about the $3\sqrt{2}$ unit cell. A vertical profile is shown in Fig. 5(c), corresponding to the line highlighted in panel (b). It is clear that the $3\sqrt{2}$ unit cell contains three protrusions, one of them with an apparent height slightly higher (about 0.1 Å) than the other two. In addition, the profile suggests that there is a dimerization of the two central protrusions. In order to quantify this effect, we calibrated the lateral scale of the images according to the $3\sqrt{2}$ periodicity, i.e., the lateral distance be-

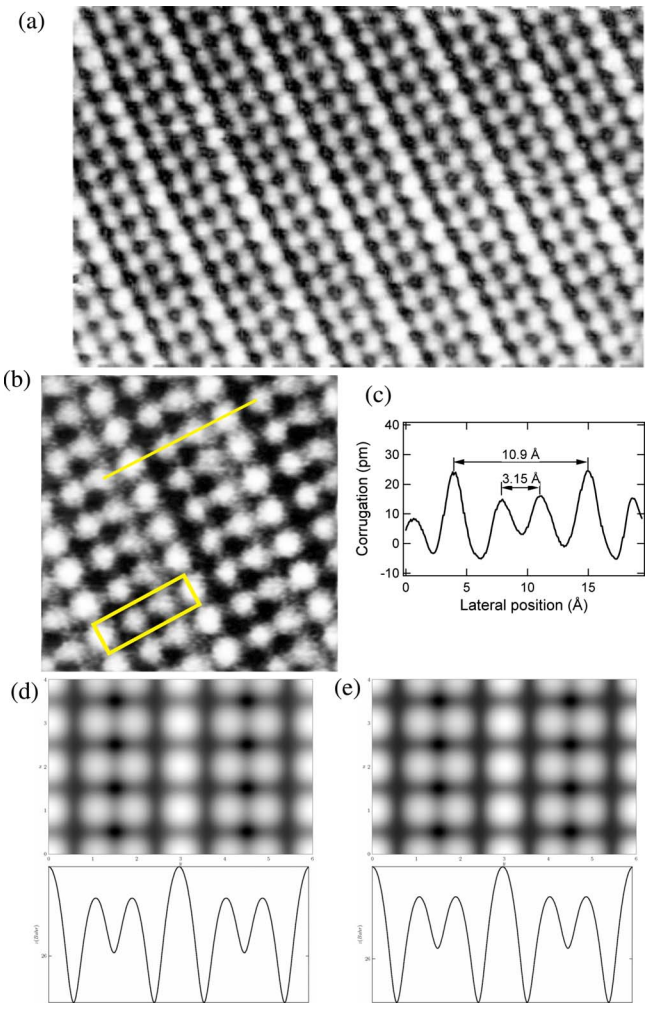

FIG. 5. (Color online) Experimental STM images of the $3\sqrt{2}$ phase compared to simulated STM images calculated for the MR structure determined theoretically in this work (see Table I). (a) Experimental filled-state image of (80×50) Å^2 taken with a bias of −0.05 V and a reference current of 2 nA. (b) Experimental filled-state image of (30×30) Å^2 taken with a bias of −0.10 V and a reference current of 2 nA. The square drawn on the image indicates the $3\sqrt{2}$ unit cell. (c) Corrugation profile of the experimental image in panel (b) along the highlighted line. Panels (d) and (e) show simulated STM images corresponding to for −0.5 and +0.5 V, respectively, together with their corresponding corrugation profiles.

tween two consecutive elevated protrusions along the direction corresponding to the $3\sqrt{2}$ periodicity was set equal to 10.9 Å. Then, we estimated from the height profile a lateral distance between the dimerized protrusions of ~3.15 Å, which is in excellent agreement with the value of 3.10 Å determined for the Sn-Sn distance in the MR structure (parameter $NN_{S_n-S_n}$ in Table I).

Figures 5(d) and 5(e) show simulated STM images of the relaxed MR structure obtained in this work for bias voltages of −0.5 and +0.5 eV, respectively. Each simulated image is accompanied by the corresponding corrugation profile. We note that the protrusions observed in the simulated images coincide with the positions of Sn atoms. A visual comparison indicates that the simulated images reproduce the main features observed in the experimental images almost perfectly, including the dimerization of the central protrusions as well as the weak dependence on the bias voltage. We therefore conclude that the protrusions observed in the experimental STM images correspond to Sn atoms. The excellent agreement between the simulated and experimental STM images is another strong evidence supporting the MR surface-alloy model for the $3\sqrt{2}$ LT phase.

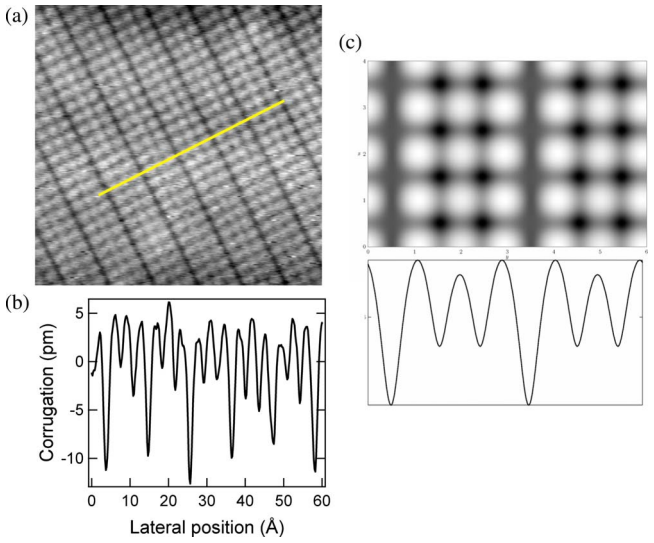

FIG. 6. (Color online) Experimental STM image of a $3\sqrt{2}$ metastable phase observed experimentally compared to a simulated STM image of the 2MR structure proposed in this work for this phase. (a) Experimental filled-state image of (82×80) Å^2 taken with a bias of −0.50 V and a reference current of 2 nA. (b) Experimental corrugation profile taken along the line indicated on the image in panel (a). (c) Simulated STM image of the relaxed 2MR structure for −0.5 V, together with its corresponding corrugation profile.

Another relevant result derived from our STM experiments on the 0.5 ML Sn/Cu(100) surface is the observation of a metastable $3\sqrt{2}$ phase coexisting with the $3\sqrt{2}$ MR structure. Figures 6(a) and 6(b) show an experimental STM image of this phase and its corrugation profile, respectively. The image exhibits a highly ordered superstructure with $3\sqrt{2}$ periodicity but, however, the superstructure does not exhibit the typical corrugation observed in the STM images of the MR $3\sqrt{2}$ phase (see Fig. 5). In fact, although the unit cell of the new $3\sqrt{2}$ phase contains three protrusions, which indicates that the Sn coverage is 0.5 ML, these protrusions have similar apparent heights in the STM image, contrary to the case of the MR $3\sqrt{2}$. Moreover, we note that the outstanding features observed in the image shown in Fig. 6(a) are channels oriented along a [001] direction, repeated with $3\sqrt{2}$ periodicity. We remark that we were able to record several consecutive images similar to this one, but this kind of structure was observed rarely and only in minute fractions of the surface. Figure 6(c) shows a simulated STM image for an applied voltage of −0.5 V of the 2MR structure obtained after relaxing the atomic positions in order to minimize the total energy. A visual comparison of this simulated image with the experimental one clearly indicates an excellent agreement. We thus attribute the $3\sqrt{2}$ metastable phase to the

2MR structure depicted in Fig. 2(c). These results strongly suggest the coexistence of the 2MR and MR phases at room temperature, which is consistent with the quite small energy difference obtained for these two structures theoretically.

IV. DISCUSSION

There are two main issues related to the crystalline structure of the $3\sqrt{2}$ phase of 0.5 ML Sn/Cu(100): first, the location of Sn atoms, forming either an overlayer or a surface alloy and second, the existence of Cu vacancies. A comparison of the theoretical results obtained for the two $\sqrt{2}$ configurations illustrated in Figs. 2(a) and 2(b) and the experimental electronic structure from Ref. 9 indicates that Sn atoms must occupy substitutional Cu sites in the top surface layer, i.e., they must form a surface alloy, since in the overlayer configuration, the Sn-Sn distance is too large to produce a surface state without the help of intermediary Cu atoms. It is worthwhile to remark here that the good agreement found between the surface band theoretically obtained for the ordered $\sqrt{2}$ surface alloy and the *S* band observed in the $\sqrt{2}$ HT phase is not a sufficient argument to conclude that the $\sqrt{2}$ phase is an ordered $\sqrt{2}$ surface alloy. Clearly, specific experimental studies oriented to investigate the structure of the HT phase are needed. The theoretical finding reported in this paper indicates that, whatever the crystalline structure is, the formation of a surface alloy is required to explain the observed surface state.

Hence, we considered for the $3\sqrt{2}$ LT phase only surface-alloy structures compatible with 0.5 ML of Sn coverage, namely, a distorted $\sqrt{2}$,[25] the MR model, and a 2MR structure. With the exception of the distorted $\sqrt{2}$ surface alloy, which turned out to be unstable, the other four analyzed structures are shown in Fig. 2, together with their corresponding Sn adsorption energies. Notice that the MR and 2MR structures are the only configurations compatible with 0.5 ML of Sn atoms, $3\sqrt{2}$ periodicity, and Cu vacancies. We found that, among the five models considered in this study, the MR surface-alloy structure has the lowest total energy and that the 2MR model, with two lines of Cu vacancies in place of one, is the next more favorable one (see Fig. 2). Very interestingly, the adsorption energies obtained for the MR and 2MR structures are significantly lower than the value obtained for the ordered $\sqrt{2}$ surface alloy by 90 and 60 meV per Sn atom, respectively, which shows that the lines of Cu vacancies play an important role in the reduction of total energy of the interface.

The comparison of the relaxed MR structure obtained in this work from total-energy-minimization calculations with different experimental results turned out to be extremely favorable for the model. First, there is an excellent agreement with the atomic structure of the $3\sqrt{2}$ LT phase determined experimentally using LEED and surface x-ray diffraction (SXRD). Second, the calculated electronic bands describe almost perfectly the main features of the surface bands observed in the $3\sqrt{2}$ LT phase using ARPES. Third, the simulated STM images reproduce the main features of the experimental STM images of the $3\sqrt{2}$ LT phase very well. On the basis of this set of strong evidences, we conclude that the $3\sqrt{2}$ MR structure describes the $3\sqrt{2}$ LT phase correctly.

A detailed knowledge of the electronic bands is needed to disentangle the mechanism driving a phase transition related to a band-gap opening. In this sense, our theoretical study provided us with an important piece of information: the empty electronic surface bands which were not measured so far. We found an empty band at the edge of the $3\sqrt{2}$ Brillouin zone with a binding energy close to the Fermi level, which we identify with a surface state. The characteristics of this band are consistent with those expected for the empty surface band that, together with the back-folded band observed at 1.45 Å^{-1} along the $\overline{\Gamma M}$ direction, would form the gap at the Brillouin-zone edge. Experiments are needed to confirm/discard the existence of this empty surface band, but an analogous band has been observed right at the Fermi energy in the related system In/Cu(100).[28] The role of this band in the electronic gapping-degapping transition is very important, as the actual gap governing the electronic entropy could be the distance between the Fermi energy and the empty surface band.[16,28]

Another important finding of this work is the experimental observation of the $3\sqrt{2}$ 2MR phase coexisting at room temperature with the ground-state $3\sqrt{2}$ MR phase. The quite small adsorption-energy difference between the MR and the 2MR structures (30 meV per Sn atom) is consistent with a coexistence of these phases at room temperature. It was not possible to determine the relative probabilities of these phases experimentally, since the 2MR phase was observed very rarely. This experimental fact suggests that at room temperature, the formation probability of the 2MR phase is small, but the observation of the two phases indicates that structures with different concentrations of vacancies can coexist at the surface. This finding is probably relevant to the interpretation of other experimental observations as well. For instance, the $3\sqrt{2}$ phase observed by Yaji *et al.*[29] in a strained Cu(100) surface might not be the ground state of the 0.5 ML Sn/Cu(100) system but the 2MR phase.

Remarkably, the existence of vacancy lines in the MR model prevents a transformation of the $3\sqrt{2}$ reconstruction into a simple $\sqrt{2}$ structure without considering some kind of atom-diffusion process in the surface. In fact, the MR $3\sqrt{2}$ unit cell contains three Sn atoms (1/2 ML), two Cu atoms (1/3 ML), and one Cu vacancy (1/6 ML) in the top layer. For the 2MR structure, there are also three Sn atoms (1/2 ML), one Cu atom (1/6 ML), and two Cu vacancies (1/3 ML). An ordered $\sqrt{2}$ surface-alloy structure with 0.5 ML of Sn atoms in substitutional Cu sites [as in Fig. 2(b)] corresponds to a 1:1 Sn:Cu ratio in the top layer. Therefore, it is not possible to obtain an ordered $\sqrt{2}$ structure with the same number of atoms in the surface as the MR $3\sqrt{2}$ one. Considering then this MR structure as the LT phase, we can think of two possibilities for the $3\sqrt{2} \Leftrightarrow \sqrt{2}$ transition: (i) an order-disorder transition, where the vacancies form a 2D gas in the HT phase; (ii) a transition where the vacancies are filled with Cu atoms in the HT phase, recovering an ordered $\sqrt{2}$ surface alloy without vacancies. In our opinion, the most probable mechanism for the transition would be the activation/deactivation of the atomic diffusion process which cause the displacements of vacancies in the top surface layer. As a

result, the $3\sqrt{2}$ periodicity would be broken giving place to a disordered surface with $\sqrt{2}$ periodicity in average, but further work is required to characterize the properties of the $\sqrt{2}$ HT phase and to understand the atomistic mechanisms involved in the phase transition, including the role of the electronic energy. In any case, there must be a surface diffusion of vacancies/atoms during the transition, indicating a more complex process than the simple distortion expected from a weak-coupling CDW transition.[29]

V. CONCLUSIONS

We conclude that a set of strong evidences supports the MR structure as the ground state of the $3\sqrt{2}$ phase, coming both from STM experiments and theoretical calculations. The calculated electronic structure of this phase is fully consistent with the experimental ARPES surface bands. We find that besides the MR structure, a 2MR phase can be observed occasionally. We propose a structural model for this phase, corresponding to a higher density of Cu vacancies in the top surface atomic layer.

ACKNOWLEDGMENTS

We thanks E. A. Sánchez for fruitful discussions. We acknowledge financial support by the following Argentine institutions: ANPCYT (Grants No. PICT2005/33432 and No. PME2003/118), Fundación ANTORCHAS, and CONICET (Grant No. PIP2009/112 200801 00958). Also, we acknowledge financial support by the Spanish Banco Santander, by MICINN (Grant No. FIS2008-00399), and by CAM (Grant No. S-0505/PPQ/0316). J.D.F, J.E.G., and H.A. are members of CONICET, Argentina.

[1] B. N. J. Persson, Surf. Sci. Rep. **15**, 1 (1992).
[2] A. Mascaraque and E. G. Michel, J. Phys.: Condens. Matter **14**, 6005 (2002).
[3] H. W. Yeom, S. Takeda, E. Rotenberg, I. Matsuda, K. Horikoshi, J. Schaefer, C. M. Lee, S. D. Kevan, T. Ohta, T. Nagao, and S. Hasegawa, Phys. Rev. Lett. **82**, 4898 (1999).
[4] R. Cortés, A. Tejeda, J. Lobo, C. Didiot, B. Kierren, D. Malterre, E. G. Michel, and A. Mascaraque, Phys. Rev. Lett. **96**, 126103 (2006).
[5] M. Minca, S. Penner, E. Dona, A. Menzel, E. Bertel, V. Brouet, and J. Redinger, New J. Phys. **9**, 386 (2007).
[6] T. Nakagawa, G. I. Boishin, H. Fujioka, H. W. Yeom, I. Matsuda, N. Takagi, M. Nishijima, and T. Aruga, Phys. Rev. Lett. **86**, 854 (2001).
[7] T. Nakagawa, H. Okuyama, M. Nishijima, and T. Aruga, H. W. Yeom, E. Rotenberg, B. Krenzer, S. D. Kevan, Phys. Rev. B **67**, 241401(R) (2003).
[8] T. Nakagawa, H. W. Yeom, E. Rotenberg, B. Krenzer, S. D. Kevan, H. Okuyama, M. Nishijima, and T. Aruga, Phys. Rev. B **73**, 075407 (2006).
[9] J. Martínez-Blanco, V. Joco, H. Ascolani, A. Tejeda, C. Quirós, G. Panaccione, T. Balasubramanian, P. Segovia, and E. G. Michel, Phys. Rev. B **72**, 041401(R) (2005).
[10] V. Joco, J. Martínez-Blanco, P. Segovia, T. Balasubramanian, J. Fujii, and E. G. Michel, Surf. Sci. **600**, 3851 (2006).
[11] C. Binns and C. Norris, J. Phys.: Condens. Matter **3**, 5425 (1991).
[12] J. Martinez-Blanco, V. Joco, J. Fujii, P. Segovia, and E. G. Michel, Phys. Rev. B **77**, 195418 (2008).
[13] V. Joco, J. Martinez-Blanco, I. Vobornik, P. Segovia, and E. G. Michel, J. Phys.: Condens. Matter (to be published).
[14] E. Tosatti, in *Electronic Surface and Interface States on Metallic Systems*, edited by E. Bertel and M. Donath (World Scientific, Singapore, 1995).
[15] G. Grüner, *Density Waves in Solids* (Addison-Wesley, Reading, MA, 1994).
[16] T. Aruga, Surf. Sci. Rep. **61**, 283 (2006); J. Phys.: Condens. Matter **14**, 8393 (2002).
[17] K. Pussi, E. Al Shamaileh, E. McLoughin, A. A. Cafolla, and M. Lindroos, Surf. Sci. **549**, 24 (2004).
[18] J. Martínez-Blanco, V. Joco, C. Quirós, P. Segovia, and E. G. Michel, J. Phys.: Condens. Matter **21**, 134011 (2009).
[19] E. McLoughlin *et al.*, Surf. Sci. **482-485**, 1431 (2001).
[20] J. Martínez-Blanco, V. Joco, P. Segovia, T. Balasubramanian, and E. G. Michel, Appl. Surf. Sci. **252**, 5331 (2006).
[21] QUANTUM-ESPRESSO is a community project for high-quality quantum-simulation software, based on density-functional theory, and coordinated by Paolo Giannozzi. See http://www.quantum-espresso.org and http://www.pwscf.org
[22] We used the pseudopotentials Cu.pw91-n-van_ak.UPF and Sn.pw91-n-van.UPF from the http://www.quantum-espresso.org distribution.
[23] J. P. Perdew, J. A. Chevary, S. H. Vosko, K. A. Jackson, M. R. Pederson, D. J. Singh, and C. Fiolhais, Phys. Rev. B **46**, 6671 (1992); **48**, 4978 (1993).
[24] J. Tersoff and D. R. Hamann, Phys. Rev. B **31**, 805 (1985).
[25] A surface alloy with $3\sqrt{2}$ periodicity was obtained from the ordered $\sqrt{2}$ surface alloy by distorting its atomic structure slightly. We note that this $3\sqrt{2}$ structure is free of Cu vacancies and could be compatible with a Peierls-type transition.
[26] X. Gao, Y. M. Zhou, S. C. Wu, and D. S. Wang, Phys. Rev. B **66**, 073405 (2002).
[27] Y. Nara, K. Yaje, T. Iimori, K. Nakatsuji, and F. Komori, Surf. Sci. **601**, 5170 (2007); J. Lallo, L. V. Goncharova, B. J. Hinch, S. Rangan, R. A. Bartynski, and D. R. Strongin, *ibid.* **602**, 2348 (2008).
[28] S. Hatta, H. Okuyama, M. Nishijima, and T. Aruga, Phys. Rev. B **71**, 041401(R) (2005).
[29] K. Yaji, Y. Nara, K. Nakatsuji, T. Iimori, K. Yagyu, R. Nakayama, N. Nemoto, and F. Komori, Phys. Rev. B **78**, 035427 (2008).